

# A Nucleon-Nucleon Interaction Consistent with Theory and Experiment\*

E. LOMON, H. FESHBACH

*Department of Physics and Laboratory for Nuclear Science, Massachusetts Institute of Technology, Cambridge, Massachusetts*

The nucleon-nucleon data are fitted by a boundary condition model interaction determined largely by theoretical forms. One- and two-pion,  $\rho$ ,  $\omega$ , and  $\eta$  meson exchange adiabatic local potentials determine the interaction outside  $r_0 \approx \frac{1}{2}\mu^{-1}$ . Only the two-pion-exchange contribution contains a degree of ambiguity measured by the parameters  $\xi$  and  $\lambda$  for the pion ladder and nucleon pair diagrams, respectively. The interaction is determined at  $r_0$  by an energy-independent boundary condition for those partial waves sensitive to the short-range interaction. A very good fit to the  $p$ - $p$  data and a good fit to the  $n$ - $p$  data below 350-MeV nucleon laboratory energy, are obtained, comparable to the best phenomenological fits. The optimum or fixed values of exchange particle masses and coupling constants corresponds to their known physical values, and the  $\lambda$  and  $\xi$  parameters optimize in their theoretical range. The value attained by  $r_0$  corresponds to that predicted by the theory of the boundary condition model. There remain 19 boundary condition parameters, freely fitted, to which the data are sensitive. These may in principle be related to pion-nucleon amplitudes. Rescattering and  $\phi$  meson exchange contributions to the potential remain to be investigated, as does the effect of coupling to inelastic channels.

## I. INTRODUCTION

It has long been known<sup>1</sup> that a field theoretical description of a scattering process can be reduced to a potential. This potential used in a Schrödinger equation generates the same asymptotic amplitude as the relativistic process. The Schrödinger wave function is a representation of the two-body component of the field theoretical amplitude, permitting the calculation of three or more body results. After the Coulomb problem, this has most often been applied to nucleon-nucleon scattering.<sup>1-6</sup> Recently this potential has been partly expressed in terms of pion-nucleon and pion-pion amplitudes through the use of dispersion theory concepts<sup>7</sup> and Mandelstam relations.<sup>8</sup>

In general this potential will be nonlocal and energy-dependent. However at long range,  $r \gtrsim \mu^{-1}$  ( $\mu$  is the pion mass,  $\hbar=c=1$ ) the theoretical interaction is dominated by adiabatic, local components.<sup>4,5,7,8</sup> For  $r \lesssim \frac{1}{2}\mu^{-1}$  both theoretical<sup>5,9,10</sup> and phenomenological<sup>11,12</sup> evidence indicate that the simpler potential forms be-

come a poor approximation, and that spin-orbit and other nonlocal terms become important. For  $r < \frac{1}{2}\mu^{-1}$  the calculation of the potential becomes both difficult and ambiguous, as nonlocal many-particle-exchange terms become important.

It has been shown<sup>13</sup> that a different, simpler representation becomes valid near the same radius. The strongly nonlocal interaction involving the exchange of many particles approximates a simple boundary condition on the Schrödinger wave function at the transition radius. It is shown that the maximally nonlocal interaction consistent with causality and  $S$ -matrix analyticity leads to energy-independent boundary conditions on the partial waves. The Mandelstam relations indicate that this condition may occur at a range in which there is two-particle exchange involving an intermediate state mass which is comparable to or lower than the initial state energy. For nucleon-nucleon scattering this occurs for two pion exchange, or at  $r \approx \frac{1}{2}\mu^{-1}$ .

In the present treatment of the values of the components of the  $\mathfrak{F}$  matrix (the logarithmic derivative of the partial wave at  $r_0$ , establishing the boundary condition) are parameters fixed by the data. In principle, using the analyticity of the model amplitudes, these parameters can be related to pion-nucleon amplitudes through crossing symmetry.

The foregoing implies a fairly well-defined program in which the goal is to compare experiment to the amplitudes obtained from a potential and boundary condition in which all relevant contributions from the dispersion integrals and restrictions of crossing symmetry are included. In following this program there has been a gradual increase in the theoretical content of the potential used. In the various stages of the model, the relative importance of the various contributions to the potential, and also the charge difference of the

\* This work is supported in part through funds provided by the Atomic Energy Commission under Contract AT(30-1)-2098.

<sup>1</sup> H. Yukawa, Proc. Phys. Math. Soc. Japan **17**, 48 (1935).

<sup>2</sup> M. Taketani, S. Machida, and S. Ohnuma, Progr. Theoret. Phys. (Kyoto) **6**, 638 (1951); **7**, 45 (1952).

<sup>3</sup> K. A. Breuckner and K. M. Watson, Phys. Rev. **92**, 1023 (1953).

<sup>4</sup> A. Klein, Phys. Rev. **90**, 1101 (1953).

<sup>5</sup> N. Hoshizaki and S. Machida, Progr. Theoret. Phys. (Kyoto) **24**, 1325 (1960); **27**, 288 (1962).

<sup>6</sup> W. N. Cottingham and R. Vinh Mau, Phys. Rev. **130**, 735 (1963).

<sup>7</sup> J. M. Charap and S. P. Fubini, Nuovo Cimento **14**, 540 (1959); **15**, 73 (1960).

<sup>8</sup> J. M. Charap and M. J. Tausner, Nuovo Cimento **18**, 316 (1960).

<sup>9</sup> Y. Nambu, Progr. Theoret. Phys. (Kyoto) **5**, 614 (1950).

<sup>10</sup> N. Fukuda, K. Sawada, and M. Taketani, Progr. Theoret. Phys. (Kyoto) **12**, 156 (1954).

<sup>11</sup> J. L. Gammel and R. M. Thaler, Phys. Rev. **107**, 291, 1337; **108**, 163L (1957).

<sup>12</sup> P. S. Signell and R. E. Marshak, Phys. Rev. **106**, 832 (1957); **109**, 1229 (1958).

<sup>13</sup> H. Feshbach and E. L. Lomon, Ann. Phys. (N.Y.) **29**, 19 (1964).

pion mass, is made manifest. With the inclusion of  $\rho$ ,  $\omega$ , and  $\eta$  exchange contributions (we have neglected the modification of the  $2\pi$  continuum at the  $\rho$  meson mass), in addition to one- and two-pion exchange, the model has arrived at the point at which it explains the data as well as any phenomenological model, *with the physical values of the parameters* where known. The results at this stage are being presented on the one hand because an accurate potential, realistic for off-the-energy-shell calculations, is useful for applications in which a third particle (including a  $\gamma$  ray) is involved. On the other hand, the present success of the theoretical elements in this approach may be a guide for theoretical work on strong interactions in the immediate future.

## II. INTERACTION, DATA AND FIT

### Discussion of Potential

Different treatments of radiative and recoil corrections have yielded varying contributions to the potential from the two-pion ladder diagram.<sup>2,3,10</sup> In our view this is an ambiguity in the theoretical potential only to be settled when more is known about high-order effects<sup>14</sup>; so we have multiplied the ladder contribution by a parameter  $\xi$ . Apart from the contribution of

nucleon pairs, when  $\xi=0$  the potential is that of T.M.O.<sup>2</sup> and when  $\xi=1$  the B.W.<sup>3</sup> result is attained.

The parameter  $\lambda$  is inserted for each nucleon pair intermediate state in a time-ordered diagram. Thus there is a factor  $\lambda$  for the one-pair terms and  $\lambda^2$  for the two-pair terms. In a strict perturbation theory of the pseudoscalar interaction<sup>4</sup>  $\lambda=1$ , but it has been argued that radiative corrections strongly suppress these contributions.<sup>3,15,16</sup> Both the small  $\pi N$   $S$ -state scattering amplitudes and partial summations in field theory indicate strong damping. Although the pion-nucleon  $S$ -state scattering lengths are small, there may well be a strong short-range interaction present.<sup>17</sup> Such an effect would change rapidly off the energy shell decreasing the accuracy of any dispersion theory extrapolation from the phase shifts to the strength of the pion-nucleon vertices in the two-nucleon problem. Thus it seems proper to treat  $\lambda$  as a parameter, which is expected to be in the range  $0 \leq \lambda \leq 1$ .

However, the one-pair and two-pair contributions to the nucleon-nucleon potential to leading order in  $(\mu/M)$  are of opposite sign and cancel strongly for  $\frac{1}{2} < \lambda \lesssim 1$ . It follows that a larger  $\lambda$  does not mean a larger contribution to the potential. Furthermore, suppression of the higher-order  $\mu/M$  terms may be required.

The potential is<sup>18</sup>

$$V \equiv V_{ST} + S_{12} \quad V_T \equiv V_2 + V_4 + V_\rho + V_\omega, \quad (1)$$

where

$$V_2(r) = \frac{1}{12} g^2 \left( \frac{\mu}{M_A} \right)^2 (\boldsymbol{\tau}_1 \cdot \boldsymbol{\tau}_2) \left[ \boldsymbol{\sigma}_1 \cdot \boldsymbol{\sigma}_2 + S_{12} \left( 1 + \frac{3}{\mu r} + \frac{3}{(\mu r)^2} \right) \right] \frac{e^{-\mu r}}{r}, \quad (2)$$

$$V_4 = \frac{(g')^4}{16} \left( \frac{\mu}{M_A} \right)^4 \left[ -\frac{24\lambda^2}{\pi(\mu r)^2} \left( \frac{M_A}{\mu} \right)^2 K_1(2\mu r) + 12\lambda \left( \frac{M_A}{\mu} \right) \frac{(1+\mu r)^2}{(\mu r)^4} \exp -2\mu r - R_1(\mu r) - \boldsymbol{\sigma}_1 \cdot \boldsymbol{\sigma}_2 R_2(\mu r) - S_{12} R_3(\mu r) \right], \quad (3)$$

where

$$R_1(x) = \frac{2}{\pi} \left\{ \boldsymbol{\tau}_1 \cdot \boldsymbol{\tau}_2 \left[ \left( \frac{12}{x^2} + \frac{23}{x^4} \right) K_1(2x) + \left( \frac{4}{x} + \frac{23}{x^3} \right) K_0(2x) \right] + \xi(3 - 2\boldsymbol{\tau}_1 \cdot \boldsymbol{\tau}_2) \left[ \left( \frac{1}{x^2} + \frac{4}{x^3} + \frac{4}{x^4} \right) K_1(x) + \left( x^{-1} + \frac{2}{x^2} + \frac{2}{x^3} \right) K_0(x) \right] e^{-x} \right\}, \quad (4)$$

$$R_2(x) = \frac{2}{\pi} \left\{ -\left[ \left( \frac{8}{x^2} + \frac{12}{x^4} \right) K_1(2x) + \frac{12}{x^3} K_0(2x) \right] + \frac{2}{3}\xi(3 - 2\boldsymbol{\tau}_1 \cdot \boldsymbol{\tau}_2) \left[ \left( \frac{1}{x^2} + \frac{2}{x^3} + \frac{2}{x^4} \right) K_1(x) + \left( \frac{1}{x^2} + \frac{1}{x^3} \right) K_0(x) \right] e^{-x} \right\}, \quad (5)$$

<sup>14</sup> A. Klein, *Progr. Theoret. Phys.* **20**, 257 (1958).

<sup>15</sup> S. D. Drell and E. M. Henley, *Phys. Rev.* **88**, 1053 (1952).

<sup>16</sup> A. Klein, *Phys. Rev.* **95**, 1061 (1954).

<sup>17</sup> H. Bethe and F. J. Dyson, *Phys. Rev.* **90**, 372 (1953).

<sup>18</sup> H. Feshbach, E. Lomon, and A. Tubis, *Phys. Rev. Letters* **6**, 635 (1961). In this reference a few parentheses were omitted in the expression for TREP, and the values of  $\xi$  for TMO and BW were confused.

and

$$R_3(x) = \frac{2}{\pi} \left\{ \left[ \left( \frac{4}{x^2} + \frac{15}{x^4} \right) K_1(2x) + \frac{12}{x^3} K_0(2x) \right] - \frac{1}{3} \xi (3 - 2\tau_1 \cdot \tau_2) \left[ \left( \frac{1}{x^2} + \frac{5}{x^3} + \frac{5}{x^4} \right) K_1(x) + \left( \frac{1}{x^2} + \frac{1}{x^3} \right) K_0(x) \right] e^{-x} \right\}, \quad (6)$$

$$V_\rho = \frac{2}{3} \mathfrak{U}^2 \tau_1 \cdot \tau_2 \left[ 1 + \frac{1}{12} (1 + 2g_\nu)^2 \left( \frac{m_\rho}{M_A} \right)^2 \left\{ 2\delta_1 \cdot \delta_2 - \left( 1 + \frac{3}{m_\rho r} + \frac{3}{m_\rho^2 r^2} \right) S_{12} \right\} \right] \frac{\exp(-m_\rho r)}{r}, \quad (7)$$

$$V_\omega = \frac{9}{4} (\mathfrak{U}')^2 \left[ 1 + \frac{1}{12} (1 + 2g_s)^2 \left( \frac{m_\omega}{M_A} \right)^2 \left\{ 2\delta_1 \cdot \delta_2 - \left( 1 + \frac{3}{m_\omega r} + \frac{3}{m_\omega^2 r^2} \right) S_{12} \right\} \right] \frac{\exp(-m_\omega r)}{r}, \quad (8)$$

and

$$V_\eta = \frac{g_\eta^2}{12} \left( \frac{m_\eta}{M_A} \right)^2 \left[ \delta_1 \cdot \delta_2 + S_{12} \left( 1 + \frac{3}{m_\eta r} + \frac{3}{(m_\eta r)^2} \right) \right] \frac{\exp(-m_\eta r)}{r}, \quad (9)$$

In Eqs. (2) and (3),  $\mu$  is to be replaced by  $\mu_{pp}$  or  $\mu_T$ , the effective pion mass for the reaction studied,  $g_\nu$  and  $g_s$  are the isovector and isoscalar gyromagnetic ratios and  $\mathfrak{U}$  and  $\mathfrak{U}'$  are the coupling constants as defined by Cottingham and Vinh-Mau.

The potential must be supplemented by the boundary conditions at  $r_0$  to determine the wave functions for  $r > r_0$ .

$$r_0(d/dr_0)u_{JS}(r) = f_{JST}u_{JS}(r_0) \quad (10)$$

and

$$\begin{pmatrix} r_0(d/dr_0)u_{J,J-1^\alpha}(r) \\ r_0(d/dr_0)u_{J,J+1^\alpha}(r) \end{pmatrix} = \begin{pmatrix} f_{J,J-1} & f_J \\ f_J & f_{J,J+1} \end{pmatrix} \begin{pmatrix} u_{J,J-1^\alpha}(r_0) \\ u_{J,J+1^\alpha}(r_0) \end{pmatrix}. \quad (11)$$

Among the parameters  $g'$ ,  $\lambda$ ,  $\xi$ ,  $r_0$  and the components of  $\mathfrak{F}$  were minimized during a computer run by one of two different search procedures. On the other hand,  $g$  (when not kept equal to  $g'$ ), the pion masses  $\mu_{pp}$  and  $\mu_T$ , the  $\rho$  mass state dependence and the nucleon-boson coupling constants were only varied from run to run (within experimental or theoretical limits); the best automatic search minimum being found for each value of these parameters attempted.

#### The Fit with Single Pion, $\rho$ , $\omega$ , and $\eta$ and Two-Pion Exchange

##### The Data Set

In most of our analysis the parameters were optimized against a set of 390  $pp$  and 257  $np$  data. Most of the data used is collected in the monograph of R. Wilson,<sup>19a</sup> with a few additions, omissions, and revisions based on subsequent data or evaluations. For computing efficiency, energies with very few data points were omitted. We have done some final fitting with the nearly complete (690 point) Signell *et al.*<sup>19b</sup>  $pp$  set. The values of  $a_{nn}$ ,<sup>20</sup> the  $^0_0 D$  state, neutron capture, and photodisintegration

results<sup>21,22</sup> were not used in fitting, but were predicted from the optimized parameters and compared with experiment.

##### The Parameters

The data were fitted to the interaction described in Eqs. (1)–(11). For  $\rho$  and  $\omega$  exchange the values  $\mathfrak{U}^2 = 0.6 - 0.65$ ,  $m_\rho = 765$  MeV,  $g_\nu = 1.83$ ,  $m_\omega = 782.8$  MeV, and  $g_s = -0.06$  were taken from the measured masses and from the analysis of nucleon form factors,  $\omega$  and  $\rho$  decay, and  $\pi$  scattering experiments.<sup>6,23</sup> On the basis of  $SU_3$  alone we chose  $\frac{3}{2}(\mathfrak{U}')^2 = 3\mathfrak{U}^2$ , taking  $\omega$  as the isospin singlet member of the vector meson octet. As the  $\eta$  is a member of the octet that includes the pions,  $SU_3$  requires

$$g_\eta^2 = \frac{1}{3} g^2 \{ 1 - [4/(1+D/F)] \}^2.$$

According to  $SU_6$   $D/F = 1.5$ . Experimental analysis of weak interactions indicates a larger  $D/F$  ratio, up to  $D/F = 2$ . We varied  $g_\eta^2$  correspondingly. The pion mass was varied in each state between its OPEP and TPEP weighted averages. The charged  $\rho$ , neutral  $\rho$  mass splitting was varied from 0–30 MeV. The parameters  $g$ ,  $g'$ ,  $\lambda$ ,  $\tau$ , and  $r_0$  were varied freely, with trials starting

<sup>19</sup> (a) R. Wilson, *The Nucleon-Nucleon Interaction* (Interscience Publishers, Inc., New York, 1963); (b) P. Signell, H. P. Noyes, N. R. Yoder, and R. M. Wright (to be published as a SLAC report).

<sup>20</sup> R. P. Haddock, R. M. Salter, M. Zeller, J. B. Czirr, and D. R. Nygren, *Phys. Rev. Letters* **14**, 318 (1965).

<sup>21</sup> F. Partovi, *Ann. Phys. (N.Y.)* **27**, 79 (1964).

<sup>22</sup> W. Bertozzi, P. T. Demos, S. Kowalski, C. P. Sargent, W. Turchinetz, R. Tallwood, and J. Russell, *Phys. Rev. Letters* **10**, 106 (1963).

<sup>23</sup> M. Carrasi and G. Pastore, *Nuovo Cimento* **27**, 1156 (1963).

TABLE I. Parameters of the BCM fit.

$g^2 = (g')^2 = 14.94$	$\lambda = 0.9343$	$\xi = 0.745$	$r_0 = 0.51373 \mu^{-1}$					
$\mu_p = 135.0 \text{ MeV}$			$\mu_1 = 137.98 \text{ MeV}$			$\mu_0 = 139.0 \text{ MeV}$		
$M_A(pp) = 938.2 \text{ MeV}$			$M_A(np) = 938.8 \text{ MeV}$			$M_A(nn) = 939.6 \text{ MeV}$		
$\mathfrak{U}^2 = 0.65$			$g_v = 1.83$			$m_\rho = 765.0 \text{ MeV}$		
$(\mathfrak{U}')^2 = 1.3$			$g_s = -0.06$			$M_\omega = 782.8 \text{ MeV}$		
$g_q^2 = 1.0$						$m_\eta = 548.7 \text{ MeV}$		

$T=1$  components of the  $\hat{f} \equiv \hat{\mathfrak{F}} + 1$  matrix:  $\chi^2 = 788$  ( $pp$  case)

uncoupled states	$^1S_0$	$^3P_0$	$^3P_1$	$^1D_2$	$^3F_3$	$^1G_4$	$^3H_5$
$f_{JST}$	1.8756	510	6.1	4.3	200	175	-4.0
Coupled states	$^3P_2 - ^3F_2$			$^3F_4 - ^3H_4$			
$f_{J,J-1}$	0.352			40.0			
$f_{J,J+1}$	20.9			-2.07			
$f_J$	-0.9			-10.83			

$T=0$  components of the  $\hat{f} \equiv \hat{\mathfrak{F}} + 1$  matrix:  $\chi^2 = 772$  ( $np$  case)

Uncoupled states	$^1P_1$	$^3D_2$	$^1F_3$	$^3G_4^a$	$^1H_5^a$
$f_{JST}$	-1.36	600	15	85	200
Coupled states	$^3S_1 = ^3D_1$		$^3D_3 - ^3G_3$		$^3G_5 - ^3I_5^a$
$f_{J,J-1}$	6.997		10.3		10
$f_{J,J+1}$	150		0.0		10
$f_J$	+31.041		6.4		10

<sup>a</sup> The data are insensitive to the core parameters in these states.

at different values near their theoretical ranges. If  $g$  approached  $g'$ , the program was run with  $g = g'$ .

*The Data Comparison*

The parameters of our  $\chi^2$  minimum are in Table I. We obtained  $\chi_{pp}^2 = 724$  for the 390  $pp$  data fitted. There were 9 free parameters (components of  $\hat{\mathfrak{F}}$ ), 3 parameters ( $\lambda, \xi, r_0$ ) bounded by theory, and one parameter  $g = g'$

known precisely from pion-nucleon experiments. In this case the degrees of freedom are  $\chi_{0,pp}^2 \geq 377$  and  $\chi_{pp}^2 / \chi_{0,pp}^2 = 1.9$ . For the 257 pieces of  $np$  data fitted we obtained  $\chi_{np}^2 = 750$ , using the 10 remaining free parameters, and the two  $\mu_T$  bounded by the charged and neutral pion masses. In this case  $\chi_{0,np}^2 \geq 245$  and  $\chi_{np}^2 / \chi_{0,np}^2 = 3.0$ .

On testing the above optimized parameters against the more extensive  $pp$  set of Signell *et al.*<sup>19a</sup> we obtained

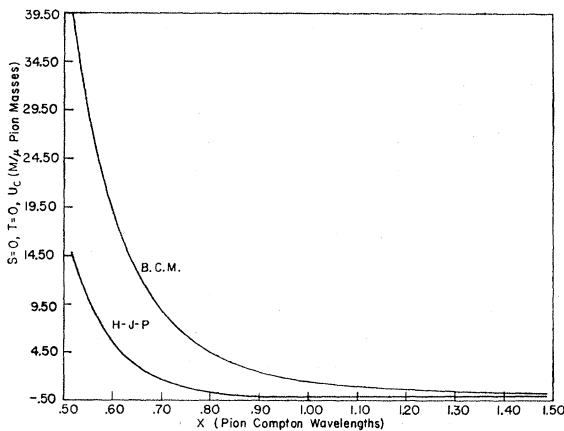


FIG. 1. The  $T=0, S=0$  central potential  $V_{00}$  of the present model is compared with that of Hamada-Johnston.<sup>24</sup> The B.C.M. potential parameters are listed in Table I. The Hamada-Johnston<sup>24</sup> parameters are the modified values used by Partovi<sup>21</sup> and Bressel,<sup>27</sup> differing but little from the original parameters. The scale of the ordinate is such that a numerical value of 1 corresponds to  $V_{00} = (\mu/M) (\mu c^2) \text{ MeV} \approx 139/7 \text{ MeV} \approx 20 \text{ MeV}$ .

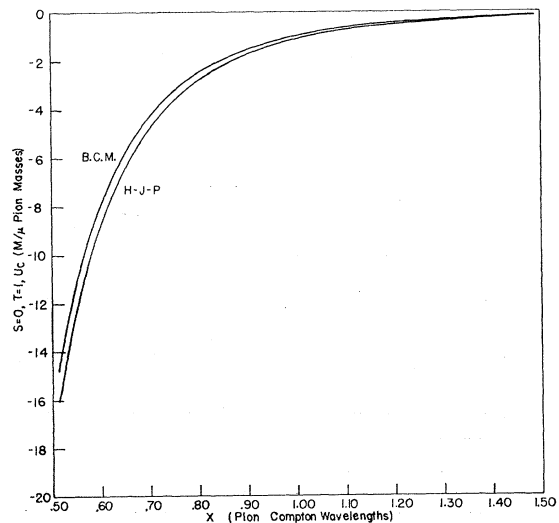


FIG. 2. The  $T=1, S=0$  central potential  $V_{01}$ , for the models described for Fig. 1.

TABLE II. Low-energy comparison.

(a) The Deuteron					
	Binding energy		Quadrupole moment		% D state
Experiment	2.2245±0.0002 MeV <sup>a</sup>		0.278±0.008 F <sup>-2</sup> b		4% <sup>c</sup>
Prediction	2.224 MeV <sup>d</sup>		0.278 F <sup>-2</sup>		5.35% <sup>e</sup>
(b) Scattering lengths					
	$a_{pp}$	$a_s$	$a_t$	$a_{nn}$	
Experiment	-7.825±0.01 F <sup>o</sup>	-23.68±0.03 F <sup>a</sup>	5.40±0.01 F <sup>a</sup>	-16.4±1.3 F <sup>f</sup>	
Prediction	-7.809 F	-23.71 F	5.42 F	-16.7 F	
(c) $p\bar{p}$ low-energy phase shifts (in degrees) <sup>g</sup>					
Energy (MeV)	0.3825	1.397	1.855	2.425	3.037
$\delta_{00}^c$ h	14.700±0.013	39.422±0.015	44.438±0.021	48.439±0.014	51.078±0.020
$\delta_{00}$	14.671	39.404	44.444	48.429	51.100
$\delta_{01}^E + 3\delta_{11}^E + 5\delta_2^{1Ei}$		-0.105±0.055	-0.045±0.085	-0.076±0.060	-0.018±0.077
$\delta_{01} + 3\delta_{11} + 5\delta_2^1$		-0.061	-0.082	-0.101	-0.111
$\delta_{01}^E i$		0.241	0.402	0.607	0.860
$\delta_{01}$		0.256	0.406	0.619	0.871
$\delta_{11}^E$		-0.146	-0.208	-0.316	-0.433
$\delta_{11}$		-0.144	-0.226	-0.340	-0.474
$\delta_2^{1E}$		0.026	0.037	0.053	0.084
$\delta_2^1$		0.023	0.038	0.060	0.088

<sup>a</sup> See Ref. 19a.

<sup>b</sup> The error is due to the different electronic wave function calculations (Ref. 19a).

<sup>c</sup> Obtained from nonrelativistic comparison with the magnetic moment (Ref. 19a).

<sup>e</sup> H. P. Noyes, Phys. Rev. Letters **12**, 171 (1964).

<sup>d</sup> Quoted to the accuracy of our eigenvalue calculation.

<sup>f</sup> See Ref. 20.

<sup>g</sup> The  $\delta_{J_S}^E$  and  $\delta_{J^{\alpha E}}$  are the phase shifts as analyzed from experiment, defined as the nuclear phase shift calculated in the presence of Coulomb

and vacuum polarization forces (Ref. e). The  $\delta_{J_S}$  and  $\delta_{J^{\alpha}}$  are calculated from our nuclear force.

<sup>h</sup>  $\delta_{00}^c$  is obtained from  $K_0$  of Ref. e by adding the correction for the presence of vacuum polarization. The correction was calculated with our exact (nuclear+Coulomb) wave functions.

<sup>i</sup> Only the weighted average  $\alpha^E$  of the  $P$  state phase shifts is determined by present experiments (Coulomb interference) (Ref. e).

<sup>j</sup> The individual  $P$  states were obtained by Noyes (Ref. e) by assuming the OPEP part of the tensor force was sufficient at these energies, and obtaining the central force contribution from  $\alpha^E$ . No errors can be quoted, but the agreement is very good compared to the errors in  $\alpha^E$ .

a  $\chi_{pp^2}/\chi_{0,pp^2}$  ratio of 4. Very minor adjustments of parameters sufficed to bring the ratio down to 2.8. The remaining discrepancy was entirely due to a few absolute differential cross sections at 20–60 MeV (we are consistently high), two integrated cross sections

near 100 MeV (low) and the addition of the old 345-MeV data at the upper end of our energy group. More substantial parameter shifts may be needed to accommodate the absolute cross sections. Work in progress has indicated only a 2.4% decrease of  $g = g'$  but

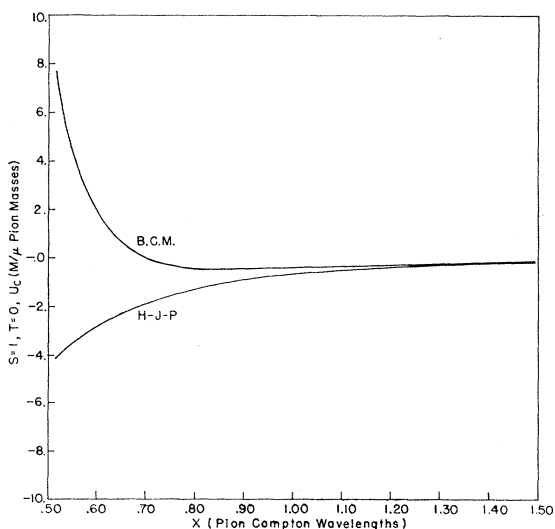


FIG. 3. The  $T=0$ ,  $S=1$  central potential  $V_{10}$ , for the models described for Fig. 1.

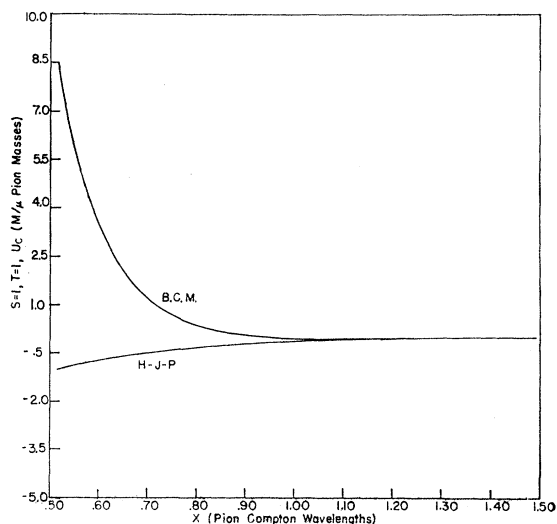


FIG. 4. The  $T=1$ ,  $S=1$  central potential  $V_{11}$ , for the models described for Fig. 1.

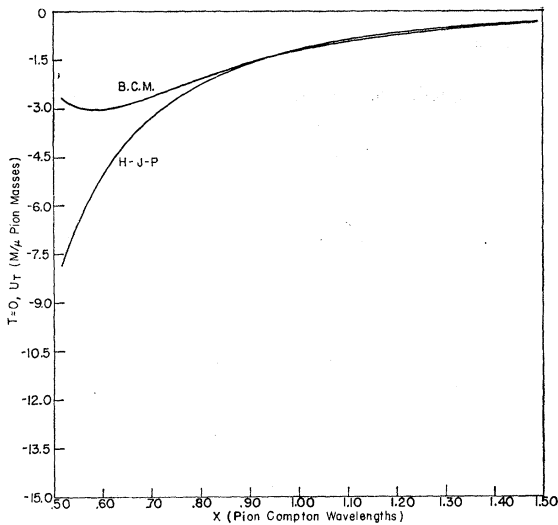


FIG. 5. The  $T=0$  tensor potential  $V_0$ , for the models described for Fig. 1.

a decrease of the ladder parameter  $\xi$  to  $\approx 0.5$ . We will here review the fit to our own data list, as slightly adjusted to obtain a  $\chi^2$  ratio of 2.8 to the Signell *et al.*  $pp$  data.<sup>19b</sup>

In Figs. 1-6 we graph our optimized potential and compare it to those of Refs. 21 and 24. The comparison of the predicted nucleon-nucleon cross sections with experimental data is shown in Figs. 7-18. The low-energy results are collected in Table II.

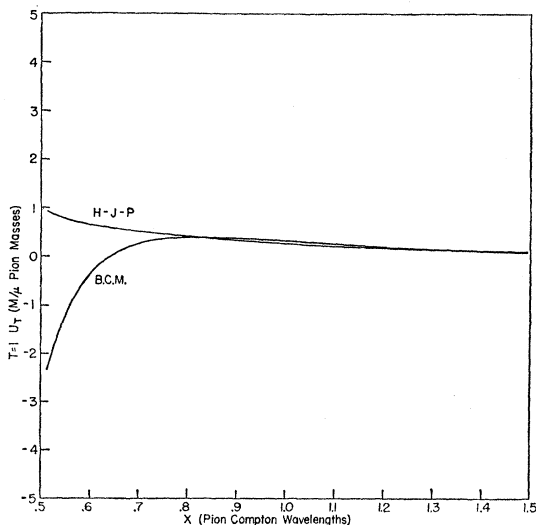


FIG. 6. The  $T=1$  tensor potential  $V_1$ , for the models described for Fig. 1.

<sup>24</sup> T. Hamada and I. D. Johnston, Nucl. Phys. **34**, 382 (1962).

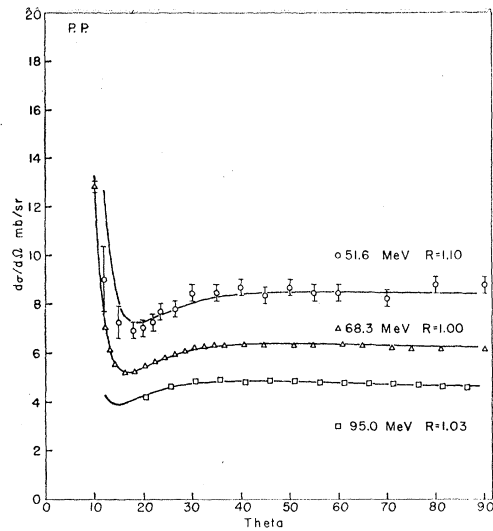


FIG. 7. The proton-proton differential cross sections at 51.6, 68.3, and 95.0 MeV. The curves are those calculated from the parameters of Table I. The experimental points are those of Ref. 19a and 19b. The normalization ratio  $R$  is the number by which the experimental mean values were multiplied.

Note that  $a_{nn}$  is satisfactorily predicted by the  $pp$  parameters simply by turning off the Coulomb and vacuum polarization interactions. Thus we satisfy charge symmetry, and also charge independence up to pion mass splitting effects. Also note that the deuteron quadrupole moment is consistent with the scattering requirements and that the 5%  $D$  state predicted is that required for the deuteron magnetic moment, without substantial meson current corrections.

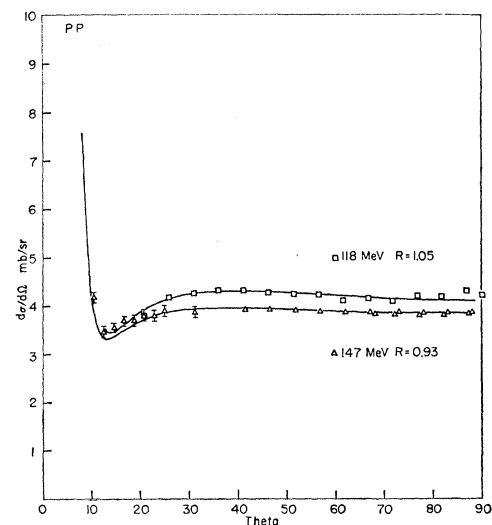


FIG. 8. The proton-proton differential cross sections at 118 and 147 MeV. Curves and points are as described for Fig. 7.

### III. DISCUSSION AND CONCLUSIONS

We have demonstrated that in the framework of the BCM the nucleon-nucleon data can be quantitatively described by a simple, theoretical form of interaction. The form includes the major part of the components expected *a priori*. All calculable theoretical restrictions on the parameters of these components are satisfied and even required by the fit. Those parameters are given in Table I.

#### The Verification of the Different Components and Parameters

The optimizing at  $g^2 \approx 15$  and  $135 \text{ MeV} < \mu < 140 \text{ MeV}$  has confirmed OPEP with precision. A 2% change in

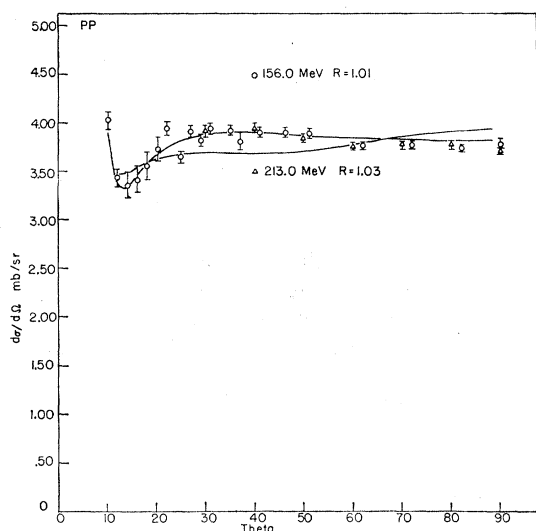


FIG. 9. The proton-proton differential cross sections at 156 and 213 MeV. Curves and points are as described for Fig. 7.

$g^2$ , or a 1% change in  $\mu$ , causes a significant change in  $\chi^2$ . It should be noted that we obtain a different (and better) value<sup>25</sup> of  $g^2$  than pure OPEC analyses.<sup>26</sup>

The over-all importance and validity of TPEP is indicated by the fact that the optimum value of  $(g')^2 \approx 15$ , determined with similar precision to the value of  $g^2$ . Except during the addition of the  $\omega$  and  $\eta$  meson exchanges, which only slightly shifted parameters,  $g^2$  and  $(g')^2$  were varied independently.

The value of  $\lambda \approx 0.9$  was stable and precise (within 0.1). This may indicate either the absence of substantial

<sup>25</sup> J. Hamilton and W. S. Woolcock, *Rev. Mod. Phys.* **35**, 737 (1963).

<sup>26</sup> M. H. MacGregor, M. J. Moravcsik, and H. P. Stapp, *Phys. Rev.* **114**, 880 (1959); M. H. MacGregor and M. T. Moravcsik, *Phys. Rev. Letters* **4**, 524 (1960).

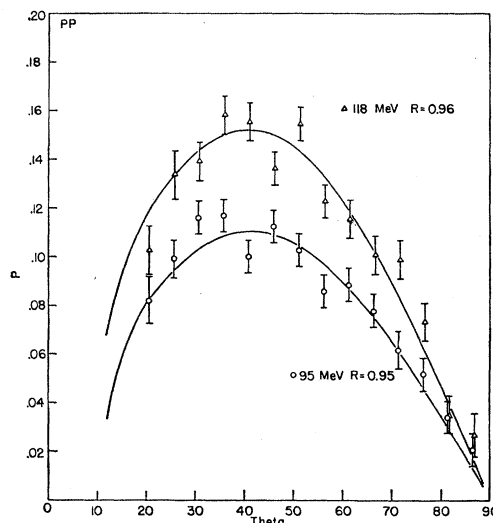


FIG. 10. The proton-proton polarizations at 118 and 95 MeV. Curves and points are as described for Fig. 7.

pair suppression or the importance of higher-order terms in  $\mu/M$ .

In the various stages of fitting with parts of the potential, the ladder parameter  $\xi$  has moved in the range  $-0.5$  to  $1.5$ . Since adding the  $\rho$  exchange it has remained between 0 and 1, but shifted importantly with the addition of  $\omega$  exchange. It is also sensitive to the data set. The present result is closer to BW<sup>3</sup> than to TMO<sup>2</sup> but the situation may easily be altered when other contributions to the theoretical potential such as rescattering and  $\phi$  meson exchange are taken into

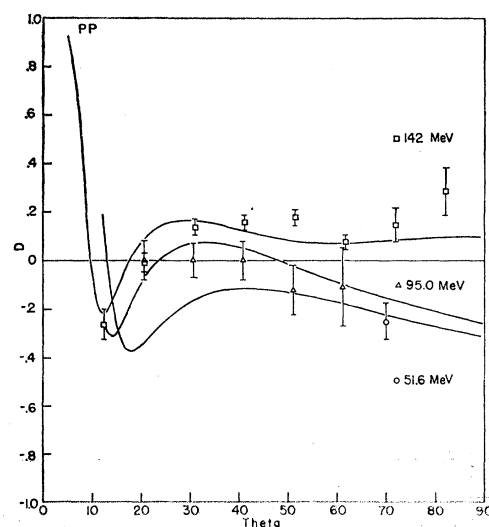


FIG. 11. The proton-proton depolarization at 51.6, 95, and 142 MeV. Curves and points are as described for Fig. 7.

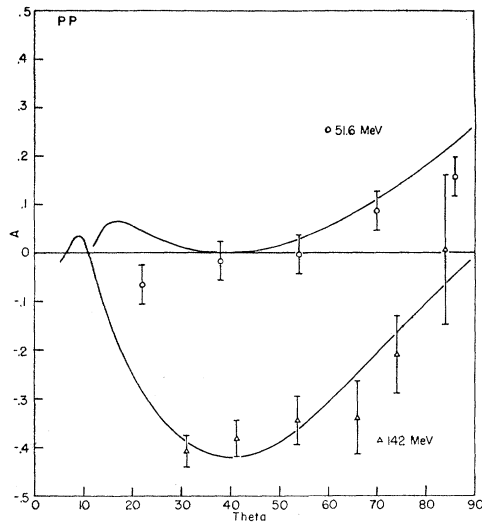


FIG. 12. The proton-proton triple scattering  $A$  parameter at 51.6 and 142 MeV. Curves and points are as described for Fig. 7.

account. But the fact that the optimal  $\xi$  does not fall outside of the BW-TMO range is again a confirmation of the validity of the TPEP contribution.

We have chosen to treat the pion masses as the same in OPEP and TPEP, for a fixed isotopic spin state. The effective TPEP average depends on  $\xi$  and  $\lambda$ . One calculation<sup>27</sup> gives the TPEP averages of  $\mu_{pp} = 139.5$  MeV,

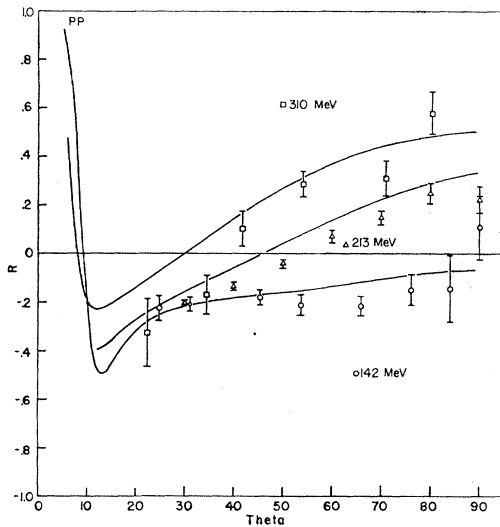


FIG. 13. The proton-proton triple scattering  $R$  parameter at 412, 213, and 310 MeV. Curves and points are as described for Fig. 7.

<sup>27</sup> C. Bressel, Ph.D. thesis, Massachusetts Institute of Technology (1965). The results are a slight alteration (to adapt to our form of potential) of those of D. L. Lin, Nucl. Phys. **60**, 192 (1964).

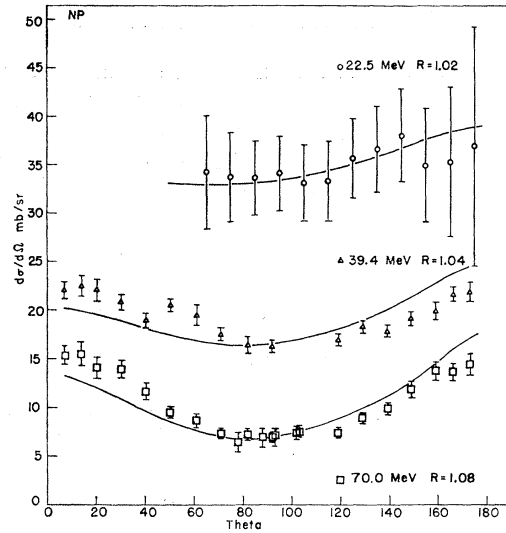


FIG. 14. The neutron-proton differential cross sections at 22.5, 39.4, and 70 MeV. Curves and points are as described for Fig. 7.

$\mu_1 = 135$  MeV and  $\mu_0 = 138.5$  MeV. The OPEP averages are unambiguously<sup>28</sup>  $\mu_{pp} = 135$  MeV,  $\mu_1 = 144$  MeV, and  $\mu_0 = 138$  MeV. The fitted  $\mu_{pp}$  and  $\mu_0$  correspond to the OPEP and TPEP values, respectively, while  $\mu_1$  is between the very different OPEP and TPEP predictions. We note that all of the charge dependence of our interaction, other than Coulomb and vacuum polarization effects, rests in these mass differences. Obtaining the correct  $a_{nn}$  is of particular significance as all param-

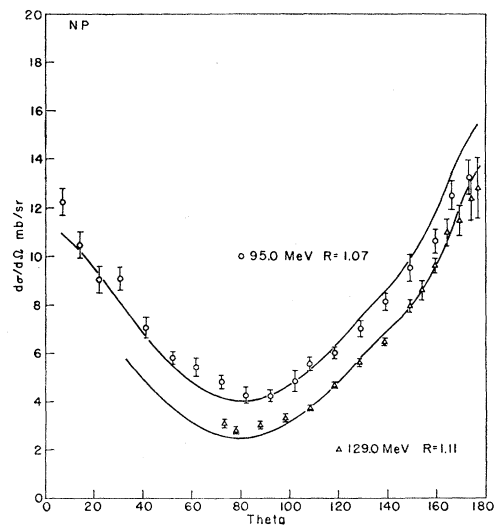


FIG. 15. The neutron-proton differential cross sections at 95 and 129 MeV. Curves and points are as described for Fig. 7.

<sup>28</sup> M. H. Hull, Jr., K. E. Lassila, H. M. Ruppel, F. A. MacDonald, and G. Breit, Phys. Rev. **122**, 1606 (1961).

eters were fixed. Thus we have been able to confirm the validity of the mass parameter in one- and two-pion exchange with unexpected precision.

Our best  $\rho$  coupling constant  $\mathfrak{N}^2=0.65$  is in agreement with the analysis of  $\pi N$  data,<sup>23</sup> and  $g_v$  was kept at the value indicated by nucleon electromagnetic form factor analysis. The large improvement in the  $np$  fit, and the movement of  $(g')^2$  to  $g^2$  [from  $(g'/g)^2 \approx 1.15$ ] indicates the importance of the  $\rho$  meson contribution. The prediction of a 4–6%  $D$  state in place of the previous 14% is also a major improvement. Our results are not sensitive to changes in the  $\rho$  mass of about 20 MeV.

The evidence for  $\omega$  exchange is slighter. Its inclusion increased the value of  $g^2=(g')^2$  by 4% putting it at the center of the range determined by the pion-nucleon

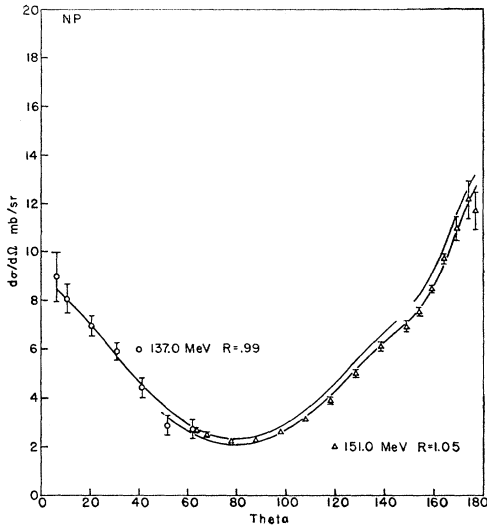


FIG. 16. The neutron-proton differential cross sections at 137 and 151 MeV. Curves and points are as described for Fig. 7.

interaction.<sup>25</sup> It decreased  $\chi_{pp}^2$  by 10% and improved the  $np$  fit to a smaller extent. We have not shown to what extent the  $\omega$  mass and  $SU_3$  octet choice of coupling are significant. Although  $(\mathfrak{N}')^2$  is three times larger than  $\mathfrak{N}^2$ , the small value of  $g_s$  compared to  $g_v$  makes the  $\omega$  exchange potential weaker than that of the  $\rho$  exchange and weakly spin-dependent. Together with its isospin independence, that makes the  $\omega$  exchange potential much less critical than the  $\rho$  exchange potential to the fit. The optimum value of  $g_s^2$  corresponds to a  $D/F$  of 1.8, in good agreement with the  $SU_3$  analysis of weak interactions.

The stability and precision of the optimizing of  $r_0=0.5 \mu^{-1}$  is a strong indication (together with the over-all goodness of fit) that the onset of an energy-independent boundary condition is a real effect, and not only a parameterization of the data. This value of

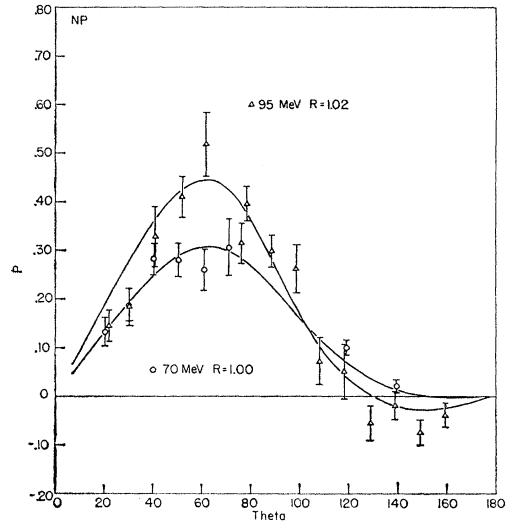


FIG. 17. The neutron-proton polarization at 70 and 95 MeV. Curves and points are as described for Fig. 7.

$r_0$  is just that required by BCM theory.<sup>13</sup> It is the largest range at which strong nonlocal and energy-dependent effects leading to a simple boundary condition arise. At the same time it is the smallest range at which both theoretical and phenomenological analysis indicate that a potential of our simple local and adiabatic form can work well. The present analysis is consistent with the hypothesis that strong interactions approach the limiting value of  $d/dk^2 (\mathfrak{F})=0$  at the lowest value of momentum transfer at which the Mandelstam double spectral function is nonzero near the elastic threshold energy.

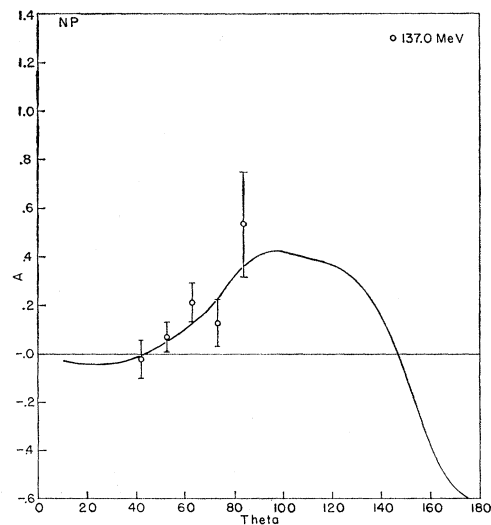


FIG. 18. The neutron-proton triple scattering  $A$  parameter at 137 MeV. Curves and points are as described for Fig. 7.

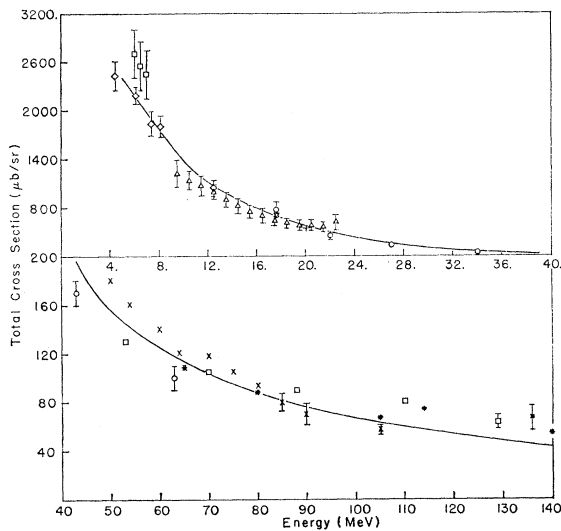


FIG. 19. The deuteron photodisintegration total cross section. The curve is computed with Partovi's program<sup>21</sup> from the potential of Table I. The data are taken from Ref. 21.

Concerning the values of the components of the  $\mathfrak{D}$ -matrix, it is to be noted that many of them are significantly different from representing nearly hard cores ( $f_{JST}$  or  $f_{JL} \gg L$ ). Several are, in fact, attractive. The model is, therefore, not a small perturbation of the usual hard core models.<sup>24,29</sup>

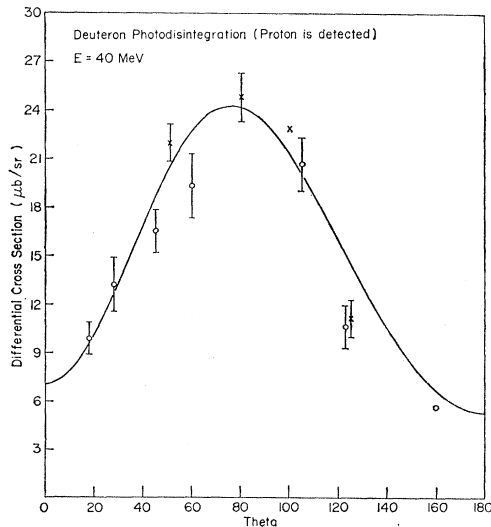


FIG. 20. The deuteron photodisintegration proton differential cross section for 40-MeV  $\gamma$  rays. The curve and data are as in Fig. 19.

<sup>29</sup> K. E. Lassila, M. H. Hull, Jr., H. M. Ruppel, F. A. MacDonald, and G. Breit, Phys. Rev. **126**, 881 (1962).

### Predictions Off the Energy Shell

The deuteron quadrupole moment,  $Q$ , is the only photon  $+2$  nucleon effect which was included in the minimizing of  $\chi^2$ . A very good value was achieved. The other static moment, the magnetic moment of the deuteron is equivalent to 4%  $D$  state in the absence of meson current effects. Our predicted result of 5%  $D$  state is consistent with the expected size of the meson current contributions. The 6–7%  $D$  state of other models<sup>24,29</sup> requires those corrections to be on the large side of all uncertainties in their calculation. The fact that the correct  $Q$  is obtained negates the OPEP argument<sup>30</sup> that a 6–7%  $D$  state is required for the experimental  $Q$ .

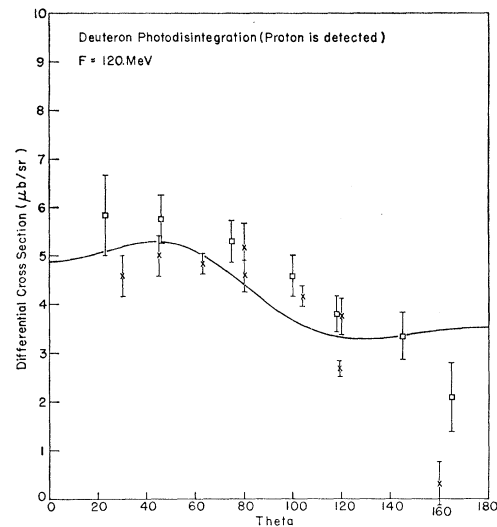


FIG. 21. The deuteron photodisintegration proton differential cross section at 120 MeV. The curve and data are as in Fig. 19.

We also predict, without any parameter variation, a satisfactory fit to the photodisintegration total and differential cross sections (Figs. 19–21). In particular the amount of isotropic component is sufficient in spite of claims that<sup>31</sup> this requires 7%  $D$  state.

Our model deuteron wave functions seems to have a definite advantage in the analysis of low momentum transfer elastic electron–deuteron scattering. With our wave functions the data yield positive values of the neutron electric form factor  $G_{En}$ .<sup>32</sup> Including the kinematic correction of Gross<sup>32</sup> the result is consistent with a straight-line extrapolation of the positive slope determined by thermal neutron scattering on electrons.

<sup>30</sup> J. Iwadare, S. Otsuki, R. Tamagaki, and W. Watari, Progr. Theoret. Phys. (Kyoto) **16**, 455 (1956); N. K. Glendenning and G. Kramer, Phys. Rev. **126**, 2159 (1962).

<sup>31</sup> J. J. deSwart and R. E. Marshak, Phys. Rev. **111**, 272 (1958); Physica **25**, 1001 (1959).

<sup>32</sup> B. M. Caspar and F. Gross (to be published).

Other wave functions, with 6–7%  $D$  state, make  $G_{En}$  too small for a reasonable extrapolation. At higher momentum transfer, in both  $e$ - $d$  elastic and inelastic scattering, the situation with respect to the consistent analysis of  $G_{En}$  and the magnetic form factor  $G_{Mn}$  is not so clear. However, fitting with our model<sup>33</sup> requires a much smaller value than other models of a presumed  $\rho\pi\gamma$  coupling, as is consistent with the nearly correct nonrelativistic static magnetic moment we predict. The  $\rho\pi\gamma$  coupling constant is experimentally too small for the other models.<sup>32</sup>

A preliminary analysis of the BCM for nuclear matter<sup>34</sup> shows that our two-body interaction has reasonable properties off the energy shell for strong interactions.

### Comparison with Other Models

The Signell *et al.*<sup>19b</sup>  $pp$  data set has been tested against other known models. Our best fit to that data set is better than that of any other model except the best boson exchange models of Scotti and Wong, to which it is equal. This situation is not changed by our fit to the very precise data at 0.3–4 MeV which is omitted from the Signell *et al.* set.<sup>19b</sup> Our  $np$  fit is as good as that of the Hamada–Johnston potential,<sup>24</sup> and better than that of the Yale potential.<sup>29</sup>

Our  $pp$  fit is much better with respect to our own data set over which almost all the minimizing was done. This implies that we may obtain a better fit to the Signell *et al.*<sup>19b</sup> data set when we have had time for a thorough search. The  $\chi_{pp}^2/\chi_{0pp}^2$  of our own data set is better than that ratio for the phase shift fits tested against the Signell *et al.*<sup>19a</sup> data. The inclusion of more absolute cross sections in the Signell *et al.* data<sup>19b</sup> will very likely prevent us from reducing our  $\chi^2$  for that data to a value equivalent to that for our own data set.

Most of the other successful models are potentials with hard cores. The OPEP part of these potentials is the only part taken from theory. The only exceptions are the Scotti–Wong<sup>35</sup> amplitudes and Bryan–Scott<sup>36</sup>

potentials based on single-boson exchanges, in which exchanged masses and coupling constants can be taken from independent experiments. The Scotti–Wong version<sup>35</sup> of that model is the only model that fits the Signell *et al.* data set as well as ours. It is noteworthy that only the single-boson-exchange models and ours are closely related to a theoretical development. This seems to indicate that our understanding of the nucleon–nucleon problem is beyond the purely phenomenological stage.

We have indicated the ambiguous elements in the relation of our model to theory. There are also ambiguous elements in the use of the single-boson-exchange model. Foremost is the neglect of the two-pion continuum exchange. Theory, even though somewhat ambiguous, gives a TPEP that is the largest contribution to the potential. It would seem to be very phenomenological to ignore it. The arbitrary  $\sigma$  meson exchange used in the single boson exchange models may be a partial replacement for the two-pion continuum, but in a phenomenological form. Other phenomenological elements in the single boson exchange models are the use of a low  $\rho$  meson mass, lack of  $\rho$  and  $\omega$  meson magnetic couplings corresponding to the form factor values of  $g_\rho$  and  $g_\omega$ , a realistic  $\eta$  meson coupling, the cutoffs, and the procedures of “unitarizing” and of adding the Coulomb effects.

The theoretical elements inherent in the single-boson-exchange model are largely incorporated into our model, the major exception being the two-pion interaction in the  $T=0$ ,  $S=0$  state, which is likely to be strong at fairly low bary-centric energy. That effect and the  $\phi$  meson should be added to our model. In addition we are considering modifications of the potential due to rescattering, higher-order recoil effects and inelasticity.

The accuracy of the model is now sufficient to consider the restrictions of crossing symmetry on the boundary conditions. That will be a considerable extension of the theoretical framework. Another direction for extension is to other baryon–baryon interactions. As the short-range forces may well be less sensitive to mass splittings of exchanged particles, it seems plausible to require  $SU_3$  or  $SU_6$  symmetry of the boundary conditions.

<sup>33</sup> B. M. Caspar, Ph.D. thesis, Cornell University (1966).

<sup>34</sup> M. M. Hoenig and E. L. Lomon, *Ann. Phys. (N.Y.)* **36**, 363 (1966).

<sup>35</sup> A. Scotti and D. Y. Wong, *Phys. Rev.* **138**, B145 (1965).

<sup>36</sup> R. A. Bryan and B. L. Scott, *Phys. Rev.* **135**, B434 (1964).